FONE: PRECISE SINGLE-TOKEN NUMBER EMBEDDINGS VIA FOURIER FEATURES

Anonymous authors

000

001

002003004

010 011

012

013

014

016

017

018

019

021

023

025

026

027

028

031

033

034

035

037

038

040

041 042

043

044

046

047

048

049

051

052

Paper under double-blind review

ABSTRACT

Language models treat numbers in the same way as ordinary word tokens, which introduces two major issues: (1) embeddings of numerical tokens primarily reflect their frequency in text corpora rather than their inherent numerical properties, leading to frequency bias, and (2) numbers are often split into multiple tokens, forcing the model to aggregate these pieces to recover their values. Inspired by the observation that pre-trained Large Language Models (LLMs) internally learn Fourier-like features for number tokens, we propose Fourier Number Embedding (FoNE), a novel method that directly maps numbers into the embedding space with their Fourier features. FoNE encodes each number as a single token with only two embedding dimensions per digit, effectively capturing numerical values without fragmentation. Compared to traditional subword and digit-wise embeddings, FoNE achieves higher accuracy on arithmetic tasks, requires significantly less training data, and offers more efficient training and inference. A 38M-parameter Transformer trained from scratch with FoNE outperforms a fine-tuned Llama-3.2-1B model on addition, subtraction, and multiplication. FoNE is also the only method that achieves 100% accuracy on over 100,000 test examples across these tasks. On 6-digit decimal addition, FoNE needs 64× less data than subword and digit-wise embeddings to reach $\geq 99\%$ accuracy, while using $3\times$ and $6\times$ fewer tokens per number, respectively.

1 Introduction

LLMs require precise representations of numerical data to perform number-related tasks effectively. However, since LLMs treat numbers just like any other token, embeddings of numerical tokens do not systematically capture important numerical features. As a result, it is challenging for even billion-parameter models to achieve perfect accuracy in solving simple arithmetic tasks ¹ (Saxton et al., 2019; Dziri et al., 2024; Lee et al., 2023; Shen et al., 2023; Zhou et al., 2023a). While generating code can be a useful workaround, relying solely on this capability highlights a fundamental limitation: without a proper understanding of numbers, the model cannot fully grasp concepts critical to domains like mathematical theorems, physics laws, or quantitative reasoning. Even with approaches like Chain-of-Thought (CoT) prompting (Wei et al., 2022), it is important to have a perfect accuracy in solving basic arithmetic tasks to build a strong foundation for more complex reasoning.

Standard tokenization approaches, such as subword tokenization (e.g., GPT-4o Achiam et al., 2023, Llama-3 (Dubey et al., 2024), Phi-2 (Abdin et al., 2024)) or digit-wise tokenization (e.g., Llama-2 (Touvron et al., 2023), Mistral (Jiang et al., 2023)), require the model to aggregate multiple tokens to understand numbers and introduces inefficiencies by tokenizing one number into multiple tokens. However, this inefficiency in tokenizing numbers leads to larger challenges when it comes to their representation. Numbers, unlike words, require systematic, frequency-agnostic representations, yet LLMs often exhibit a frequency bias (Razeghi et al., 2022; Shrestha et al., 2025; Shao et al., 2025), predicting numbers based on training data prevalence rather than their mathematical properties.

We draw inspiration from interpretability analyses of LLMs, which reveal that models internally develop Fourier-like features. Specifically, pre-trained models embed number tokens using a sparse

¹Our evaluation (See Appendix E.1) of recently released LLMs on arithmetic confirms this limitation: they still struggle with multi-digit addition and multiplication.

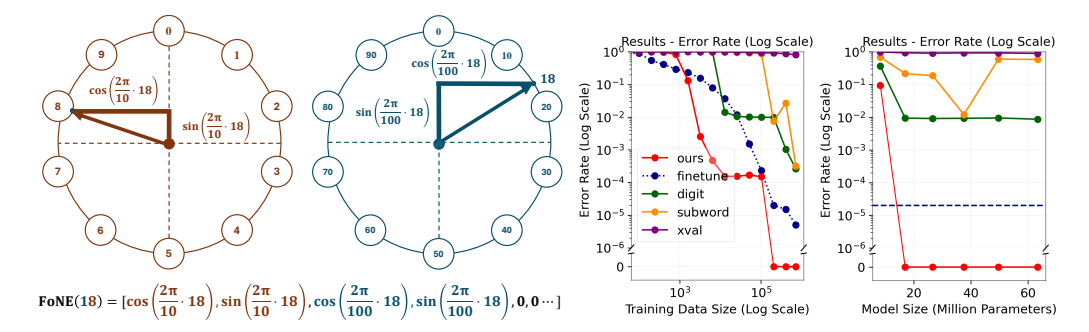


Figure 1: Overview of Fourier Number Embedding (FoNE). Left: FoNE encoder illustrated with the token '18', directly mapped into its FoNE. Middle: Test error on 6-digit decimal addition as the size of the training set increases. Right: Test error on the same task as model size increases. In both plots, we train transformers from scratch with different embedding or tokenization methods until convergence and report the final error. We compares FoNE (ours) against digit-wise tokenization, subword tokenization, XVAL (Golkar et al., 2023), and a fine-tuned Llama-3.2-1B model. FoNE achieves higher accuracy with less data and model size, even surpassing the finetuned Llama baseline

set of features in the Fourier domain (Zhou et al., 2024). These features enable the representation of numbers capturing both the magnitude and exact values of numbers, which are critical for solving arithmetic tasks (Zhou et al., 2024). However, because numbers are split into subwords and their embeddings are learned from co-occurrence statistics in text during pre-training, current LLMs fail to learn precise numerical representations and struggle to extend these mechanisms to larger numbers, underscoring the need for more systematic approaches to numerical representation.

In this paper, we propose a novel approach called Fourier Number Embedding (FoNE), which directly maps numbers to their Fourier representations, bypassing the tokenization step entirely. By representing each digit using *cosine and sine functions with different periods*, as shown in the left panel of Figure 1, FoNE ensures precise representation of numbers. FoNE represents each digit using only two dimensions in the embedding vector. This compact design not only reduces computational overhead but also creates opportunities for future extensions by incorporating additional features to better capture numeric properties. By embedding and predicting numbers directly as single tokens, our method eliminates the need for multiple forward passes and token aggregation, significantly enhancing computational efficiency. Furthermore, we provide a theoretical justification for why FoNE can represent numbers accurately as single tokens, leveraging the modular encoding properties of trigonometric functions to ensure exact recovery of each digit through periodic embeddings.

Beyond theoretical justification, we demonstrate the effectiveness of FoNE through extensive experiments on arithmetic tasks, including addition, subtraction, and multiplication. Our results show that FoNE is the only approach which—when used to train a Transformer from scratch—achieves perfect accuracy on multiple arithmetic tasks while requiring significantly less training data and fewer model parameters compared to existing methods. Moreover, FoNE offers faster training and inference times by encoding each number into a single token. On 6-digit decimal addition it achieves $\geq 99\%$ accuracy using $64\times$ less data than subword or digit-wise embeddings, while cutting token usage per number by $3\times$ and $6\times$, respectively. These findings underscore FoNE's capacity to represent and manipulate numerical data both efficiently and precisely within large language models.

2 Related Work

Arithmetic and Number-Related Tasks in LLMs. Using language models for number-related tasks, including solving math problems (Saxton et al., 2019; Yu et al., 2023; Meidani et al., 2023), time-series prediction (Tan et al., 2024; Ma et al., 2024; Zhou et al., 2023b; Liu et al., 2024a; Jin et al., 2023; Cao et al., 2023; Li et al., 2025), quantitative reasoning (McLeish et al., 2024b; Liu et al., 2024b; Chen et al., 2023; Jin et al., 2024; Cobbe et al., 2021), and handling tabular data (Gao et al., 2024; Fang et al., 2024; Sahakyan et al., 2021), remains a significant challenge. Despite advancements in transformer-based models, LLMs such as Qwen3-235B and GPT-5, with billions of parameters, struggle to solve simple arithmetic problems involving multi-digit addition and multiplication across multiple forward passes (Dziri et al., 2024; Feng et al., 2024), even when using scratchpads (Nye et al., 2021).

Golkar et al. (2023); Sundararaman et al. (2020); Jiang et al. (2019); Sivakumar & Moosavi (2024), introduce number embedding methods to enhance model performance on number-related tasks. However, the range of numbers these methods can accurately represent is typically limited to fewer than five digits and fail to achieve perfect accuracy. Additionally, a line of research (McLeish et al., 2024a; Shen et al., 2023) incorporates the positional information of digits into embeddings or adds it as extra tokens (Nogueira et al., 2021). Lee et al. (2023) demonstrate that smaller transformer models can successfully handle multiplication when equipped with carefully designed scratchpads. However, these approaches are tailored specifically for arithmetic tasks and are difficult to integrate seamlessly into general-purpose LLM training. Thawani et al. (2021) explores encoding strategies like digit-by-digit, scientific notation, and base-10 formats, while Jiang et al. (2019) maps numbers to finite "prototype numerals". These methods help the model align digits of equal significance but often require digit-wise tokenization and introduce additional tokens, reducing training and prediction efficiency. In contrast, the method proposed in this paper precisely encodes all numbers as a single token, eliminating range limitations and avoiding the efficiency drawbacks associated with previous approaches (see Section 5 for further details).

3 METHODS

Building on insights from prior studies (Zhou et al., 2024) that highlight the importance of Fourier features in numerical embeddings, we propose Fourier Number Embedding. Unlike existing methods that often require digit-wise tokenization or pre-training to handle numeric tasks, FoNE directly maps numbers into compact Fourier representations. Sections 3.1, 3.3, and 3.4 describe our embedding, decoding, and integration methods, respectively. The complete process is shown in Figure 2.

3.1 FOURIER NUMBER EMBEDDING (FONE)

We first introduce the following function that maps each $x \in \mathbb{R}$ to a point on the unit circle.

Definition 3.1 (Circular embedding). Let T be a given period. We define the function $\phi: \mathbb{R} \to \mathbb{R}^2$ as

$$\phi(x,T) := \left(\cos\left(\frac{2\pi}{T}x\right), \sin\left(\frac{2\pi}{T}x\right)\right).$$

Next, we formally define FoNE, which directly maps any floating point number x to an embedding. We predefine m and n as the maximum number of digits before and after the decimal point, respectively.

Definition 3.2 (Fourier Number Embedding). Let m be the integer digit length, and n be the decimal digit length. We define the Fourier Number Embedding function $FoNE : \mathbb{R} \to \mathbb{R}^{2(m+n)}$ for an input number x as follows:

$$FoNE(x, m, n) := [\phi(x, T_{-n+1}); \phi(x, T_{-n+2}); \dots; \phi(x, T_m)],$$

where $T_i = 10^i$ for each integer i in the range -n + 1 to m.

To align the embedding dimensions of FoNE with the model's input embedding dimension d, we map the Fourier Number Embedding, which lies in $\mathbb{R}^{2(m+n)}$, to \mathbb{R}^d . This mapping can be achieved in two ways: (1) by applying a learnable linear transformation $\mathbf{W} \in \mathbb{R}^{d \times 2(m+n)}$, or (2) by appending zeros to the embedding vector to match the dimensionality d. As demonstrated in Section 4.3, both approaches achieve comparable results.

3.2 FONE'S REPRESENTATIONAL PROPERTIES

Then, we introduce an elementary lemma and demonstrate why FoNE can preserve the numeracy on numbers.

Lemma 3.3 (Informal version of Lemma D.1). Given the pair $\left(\cos\left(\frac{2\pi}{T}x\right),\sin\left(\frac{2\pi}{T}x\right)\right)$, we can recover $x \mod T$.

Hence, by applying Lemma 3.3 to each frequency component in FoNE, we immediately obtain the following result.

Lemma 3.4 (FoNE preserves numeracy). Given a number's Fourier Number Embedding FoNE(x), its integer digit length m, and the decimal digit length n, by using Lemma 3.3, we can recover $x \mod 10^i$ for each integer i in the range -n+1 to m.

A natural question that arises here is the need for $x \mod 10$, if we already know $x \mod 100$. The reason is that even though knowing $x \mod 100$ exactly suffices to recover $x \mod 10$, this estimation is noisy in practice. When T becomes very large in a circular embedding (Definition 3.1), the difference $\frac{2\pi}{T}(x+1) - \frac{2\pi}{T}x$ approaches zero, causing the embedded representations of x and x+1 to become arbitrarily close on the unit circle. Consequently, a single large T cannot sufficiently distinguish adjacent values in the embedding. Hence, one must choose T across a broad range of scales to ensure that the embedding remains adequately distinguishable for all values of x. In this paper, we choose T as 10^i , $\forall i$, so that each T effectively captures one digit of x.

To provide a clear illustration of our method, we present a detailed example demonstrating how we map number 4.17 to its embedding.

Example 3.5. Consider x = 4.17. Its Fourier Number Embedding is given by

$$[\phi(4.17, 0.1); \phi(4.17, 1); \phi(4.17, 10)],$$

where ϕ is defined in Definition 3.1. From these components, by using Lemma 3.3, we can recover

$$[4.17 \mod 0.1, 4.17 \mod 1, 4.17 \mod 10],^2$$

which simplifies to [0.07, 0.17, 4.17]. If we used only T=10, then $\phi(4.17, 10)$ would be nearly indistinguishable from $\phi(4.18, 10)$, causing the embedding to lose fine-grained information about less significant digits. However, with these chosen periods T, we can capture all the digits.

3.3 DECODING

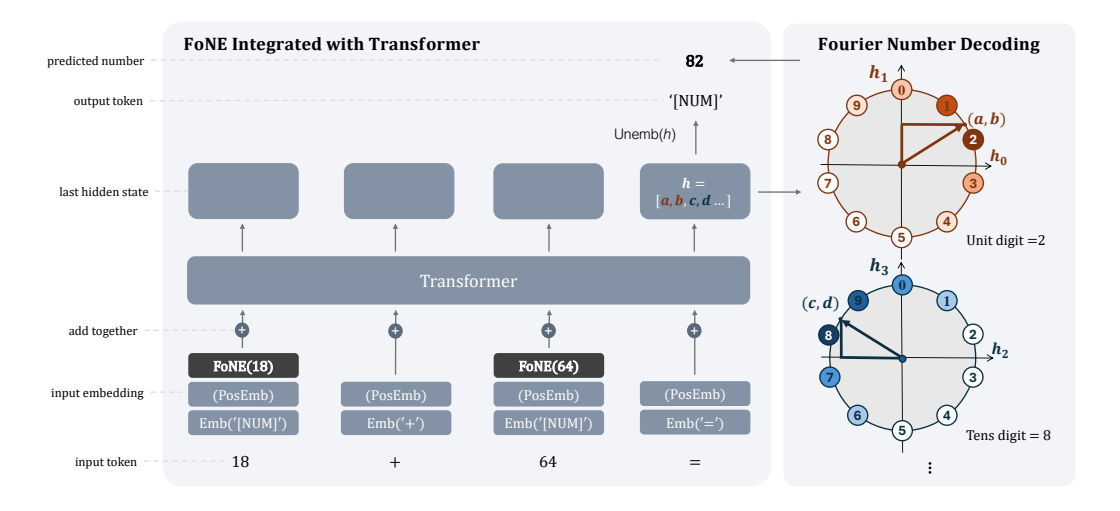


Figure 2: Left: Each number in the input sequence is replaced by a special token [NUM] and embedded as the sum of [NUM] token embedding, its FoNE (see Figure 1(a)), and the standard position embedding (if used by the architecture; Llama-3.2 does not use an explicit position embedding). Right: At decoding time, every pair of hidden-state entries corresponds to one digit, e.g. the first two entries h_0 and h_1 correspond to the unit digit. The model identifies the digit whose circular Fourier representation best matches those two entries. Digits are then combined by their positional weights.

As each number has its own FoNE, calculating the logits for all possible numbers becomes computationally infeasible. Therefore, we introduce a novel decoding head that maps hidden states from Fourier space to number space as shown in Figure 2. Below, we explicitly define the loss function and prediction function for each digit and then show how to combine these to obtain the final loss and prediction.

²For real x and positive real m, x mod m is defined as $x - m \cdot \left| \frac{x}{m} \right|$, yielding a value in the range [0, m)

Definition 3.6 (Fourier Number Loss Function). Let $h \in \mathbb{R}^d$ denote the last-layer hidden state of the model. Let y_i denote the i-th digit of the label number y. Let L_{CE} denote the cross entropy loss. For digit i, we define the Fourier Number Loss Function L_{FoNE} as:

$$L_{\mathsf{FoNE}}(h,y,i) := L_{\mathsf{CE}}\Big(y_i, \underbrace{([h[2i],\ h[2i+1]]}_{1\times 2} \cdot \underbrace{[\phi(0,10);\cdots;\phi(9,10)]^\top}_{2\times 10})\Big).$$

This construction allows each digit to be treated as a separate prediction task while sharing the same underlying model representation h. By taking the average of $L_{\sf FoNE}(h,y,i)$ over all digit positions i, we obtain the final training loss.

Definition 3.7 (Fourier Number Prediction for the *i*-th digit). Let $h \in \mathbb{R}^d$ denote the last-layer hidden state of the model. For digit *i*, we define the Fourier Number Prediction as:

$$\widehat{y}_i := \arg \max_{j \in \{0, \dots, 9\}} ([h[2i], h[2i+1]] \cdot [\phi(j, 10)]).$$

Here, \hat{y}_i is determined by the similarity between the hidden states and the circular embedding of number in $\{0, \dots, 9\}$ as illustrated in Figure 5(d). Once we have computed \hat{y}_i for each digit i, the final prediction for the entire number can be formed by concatenating these digit-wise predictions. We defer the detailed algorithms to Appendix A.

3.4 Incorporating FoNE into Input Sequences

To incorporate FoNE, we create one special token <code>[NUM]</code> and add it to the vocabulary. This token must be generated by the model in order to generate any number. We can then remove any tokens corresponding to numbers from the vocabulary. The integration of FoNE into input sequences proceeds as follows, as illustrated in Figure 2 and Figure 5:

- 1. Extract all numbers from the input sequence to create a number list. Replace each number with [Num] and tokenize the sequence to obtain a token list.
- 2. Embed the token list using standard word embedding methods.
- 3. Map each number in the number list to FoNE representation using Algorithm 1 (Section 3.1).
- 4. Add the FoNE to the word embedding of the corresponding [Num] token.
- 5. Feed the combined embeddings into the model.
- 6. Use the model's output embeddings to predict the next token in the sequence.
- 7. If the predicted token is [Num], decode the numerical value using the method described in Section 3.3, or compute the loss during training.

This procedure ensures that FoNE embeddings are seamlessly integrated into the input sequence, enabling the model to leverage both numerical and contextual information effectively.

4 EMPIRICAL EVALUATION

4.1 EXPERIMENTAL SETTING

We evaluate the performance of our proposed *FoNE* method on arithmetic tasks designed to benchmark different number embedding methods. The dataset includes tasks such as 6-digit integer addition, 6-digit decimal addition (with 3 digits after the decimal), 5-digit integer subtraction, 3-digit integer multiplication, and 4-digit integer multiplication. These tasks are curated to measure model capabilities in accurate numeric computation, while remaining within ranges where baseline embedding methods are still competitive—since their performance degrades rapidly for larger numbers. To further probe the scalability of our approach, we additionally evaluate FoNE on 60-digit addition in Section 4.4, which highlights its ability to handle much larger operands where other embeddings fail.

Dataset. Each example in the dataset is formatted as [operand a] [operator] [operand b]=, where the operands a and b are sampled based on the operation type. For addition and multiplication, we ensure $a \le b$ to avoid duplication (e.g., a+b and b+a are treated as identical and included only once). For subtraction, we enforce $a \ge b$ to ensure non-negative results. For an x-digit operands dataset, each operand can have up to x digits. The dataset is divided into training, validation, and test subsets as shown in Table 9 in Appendix I.

Baselines. We compare our proposed FoNE method against several baseline methods for numeric embeddings. First, we consider digit-wise tokenization, where each digit in a number is treated as an individual token. Second, we evaluate subword tokenization, where numeric values are tokenized into subword units based on the Llama3.2-1b tokenizer's default vocabulary. Third, we include the xVAL method Golkar et al. (2023), which leverages explicit value-based representations for numeric computation. As xVAL predict floating point numbers, predictions are rounded to calculate accuracy. Finally, we fine-tune pre-trained LLMs on the same dataset for comparison.

Setup. Our experiments involve multiple configurations of randomly initialized transformer-based models. Models were evaluated across varying sizes, ranging from small to large architectures as defined in Table 11. For the accuracy vs. training data size experiments, we use a configuration similar to Llama-3.2 but with 38M parameters. In Appendix J, we conduct more experiments on a transformer model with a different configuration and observe consistent results.

Learning rates were determined through an extensive search, with the best rates selected separately for each method based on the validation performance. Model evaluation used exact match accuracy to assess numeric prediction correctness. All models were trained from random initialization, except the fine-tuned Llama-3.2-1B baseline model. We varied the training data size by uniformly sampling subsets and adjusted model sizes to compare accuracy across methods.

4.2 EXPERIMENT RESULTS

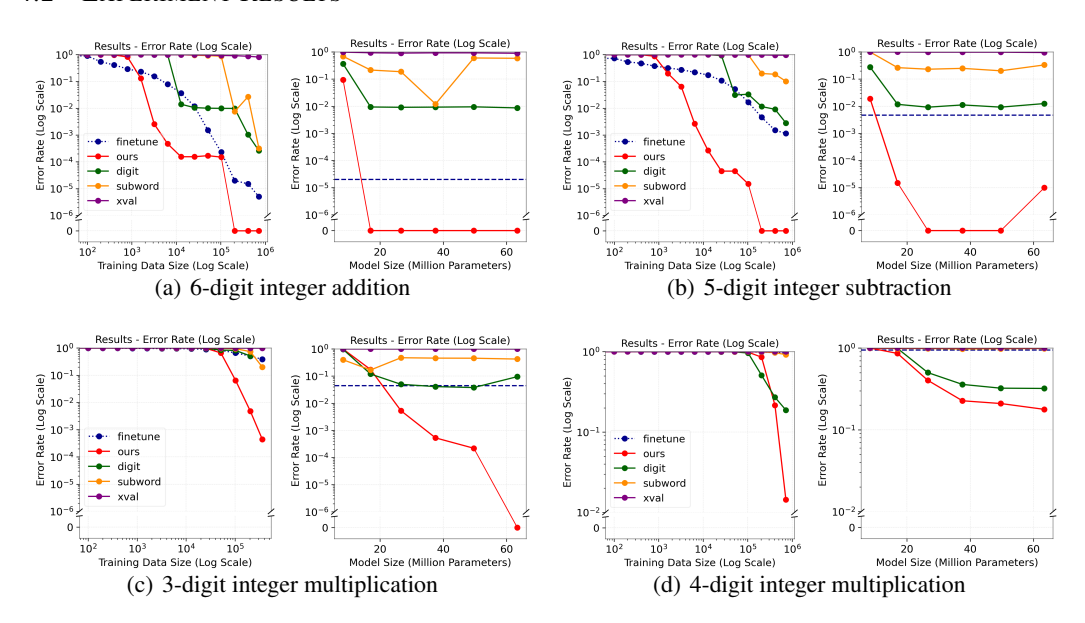


Figure 3: Comparison of accuracy for various arithmetic tasks with respect to model and data size.

Data Efficiency. The middle panel of Figure 1 illustrates the accuracy trends of different embedding methods as the data size increases for the 6-digit decimal addition task. Remarkably, our model achieves 99% accuracy with just 6,400 training samples and 37.55 million parameters, requiring $64 \times$ less training data than traditional embedding methods (409,600/6,400=64). Even with only 3,200 training samples, our method outperforms the fine-tuned Llama-3.2 model. Additionally, it achieves perfect accuracy with 51,200 training samples.

Beyond synthetic tasks, our approach also improves compute efficiency in real-world scenarios. For instance, FoNE requires only 149.25 tokens on average to represent numerical values from a table in the WikiTableQuestions dataset (Pasupat & Liang, 2015), compared to 329.7 tokens used by a digit-wise tokenizer. This significant reduction in token usage highlights the efficiency of our method in encoding numerical data, making it more scalable for number-heavy tasks.

Parameter Efficiency. The right panel of Figure 1 shows the accuracy trends of different embedding methods as the model size increases for the 6-digit decimal addition task. Our method achieves 97%

accuracy with just 1 layer and 8.31 million parameters using 200k examples for training. Furthermore, with 26.62 million parameters, it surpasses the fine-tuned Llama-3.2 model and achieves 100% accuracy.

Different Tasks. We conducted the same experiments across all different datasets. As shown in Figure 3, our method consistently demonstrates superior data and parameter efficiency compared to other approaches. Notably, it is the only method that achieves perfect accuracy on 6-digit decimal addition, 6-digit integer addition, 5-digit subtraction, and 3-digit multiplication. We also show that our method performs better in a binary classification task that involves numerical values in Figure 6 and Figure 7. Specifically, the task requires predicting a label based on a linear equation applied to three integers. In addition, we evaluate FoNE on a modular addition task. In Table 6, we show that it outperforms standard tokenization methods, especially under large moduli where conventional approaches fail. Due to space limitations, we defer the details to Appendix B.

Training and Inference Efficiency. Table 1 compares the training and test times used for one epoch across different embedding methods. Our method is consistently faster than digit-wise and subword embedding methods, as it uses one token to embed each number. Compared with XVAL, our method consistently achieves higher accuracy. Additionally, we show the number of tokens required to tokenize the maximum number for different methods, highlighting the efficiency of our approach.

Table 1: Training and inference efficiency comparison across three arithmetic tasks. The times are reported in minutes (') and seconds (").

	De	ecimal	Addition	1		Subtra	action		N	Iultipl	ication	
Method	Train Time	Test.	Tokens	Accuracy	Train.	Test.	Toks.	Acc.	Train.	Test.	Toks.	Acc.
Ours	3'18"	29"	1	100	2'42"	29"	1	100	2'56"	33"	1	98.56
Digit-wise	11'48''	1'25"	7	99.85	9'41''	1'15"	5	99.71	10'11''	1'18''	8	81.21
Subword	6'46''	58''	3	97.94	5'47''	54"	2	91.66	6'20''	58"	3	8.05
XVAL	3'17"	27''	1	0.44	2'54"	27"	1	3.41	2′56′′	$26^{\prime\prime}$	1	0

4.3 ABLATION STUDIES

Linear Layer after FoNE. As discussed in Section 3.1, we evaluate the use of a linear layer applied after FoNE and compare it with the approach of appending zeros to align the embedding dimensions with the model's input requirements. As shown in Table 2, both configurations achieve almost the same accuracy. Hence, either technique can be used to align FoNE with the embedding dimension.

Table 2: Accuracy Comparison Across Datasets

Table 3: Accuracy Comparison Across Periods

Task	Linear	Zero Padding	Dataset	2,5,10	10	5	7
Decimal Addition	100%	100%	Decimal Ad	dition 100	100	1.52	3.64
Integer Addition	100%	100%	Integer Add	ition 100	100	1.55	0.02
Multiplication	99.95%	99.91%	Multiplicati	on 99.99	99.95	3.67	1.91
Subtraction	100%	100%	Subtraction	100	100	4.64	0.24

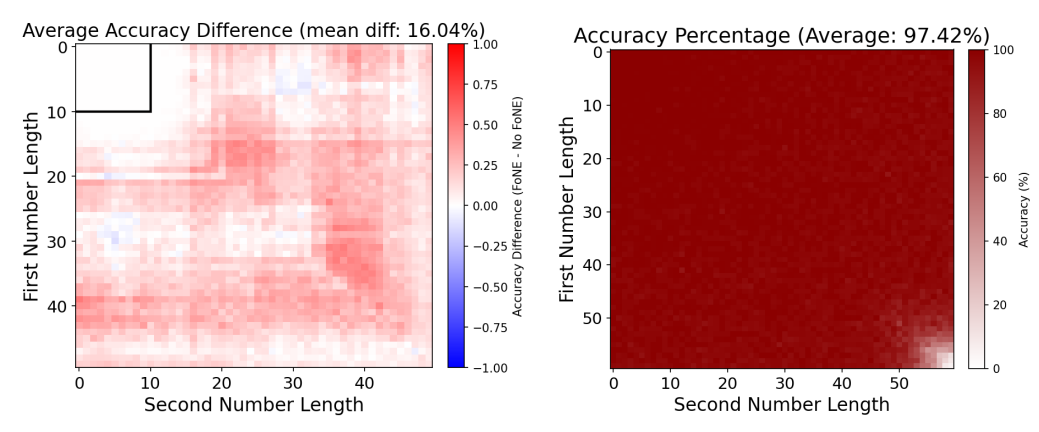
Effect of Different Periods. As discussed in Section 3.1, the modular group captures the necessary information for each digit, ensuring the effectiveness of our approach. We test the model with base periods of [2,5,10], [5], and [7], as shown in Table 3. The [2,5,10] configuration achieves accuracy comparable to that of the 10-period setup across different datasets. In this paper, we choose single 10 to make it more parameter efficient. However, configurations using only $\mod 5$ or $\mod 7$ exhibit significantly lower accuracy. This is because neither $\mod 5$ nor $\mod 7$ can fully represent the required information for all digits.

The mispredictions are attributed to the absence of critical modular information. As illustrated in Table 12 in Appendix I, in the decimal addition task, using only a mod5 representation prevents the model from distinguishing between certain digits, such as 2 and 7, which results in errors.

Necessity of Sine and Cosine Encoding. A natural question arises: are sinusoidal encodings truly necessary for arithmetic tasks? One could directly encode each digit into a separate dimension of

the embedding, representing a number like 567 as [5,6,7]. However, this approach fails to achieve perfect accuracy. For instance, numbers such as 999 and 888 become nearly indistinguishable after layer normalization, which reduces their differences and can lead to confusion during training. We evaluate this direct encoding method on 6-digit decimal addition and, after performing a learning rate search, find that the best accuracy is 99.3% with a learning rate of 0.01 and training for 100 epochs. In contrast, FoNE achieves better accuracy in just 6 epochs with the same dataset and model size. This suggests that naive direct encoding does not adequately preserve numerical distinctions for reliable arithmetic operations. As illustrated in Table 13 in the appendix, the model frequently mispredicts 8 as 9, further demonstrating the limitations of direct encoding in preserving numerical structure.

4.4 APPLICATIONS AND COMPLEMENTARITY OF FONE



(a) Impact of combining FoNE with Abacus embedding (b) Test accuracy of 60-digit addition with FoNE

Figure 4: (a) Performance improvements achieved by combining FoNE with the Abacus embedding method across various random seeds. The transformer is trained on addition tasks with up to 10-digits numbers (represented by the smaller square) and tested up to 50-digit numbers. (b) Average accuracy of an 8-layer transformer model on 60-digit addition tasks using FoNE for chunked input.

Combining FoNE with Abacus. FoNE can be combined with other positional embedding methods even with different tokenization methods, requiring only minor modifications. For instance, we integrated FoNE with the Abacus embedding method (McLeish et al., 2024a), which operates on digit-wise tokenization. In this setup, the embeddings for each digit (0–9) are replaced with their corresponding FoNE. We trained an 8-layer transformer model on integer addition tasks with up to 10 digits and tested it on addition tasks involving up to 50-digit numbers. The results, as illustrated in Figure 4(a) and Figure 11 in Appendix G, show that incorporating FoNE consistently improves the performance of the Abacus method across various random seeds. This highlights the complementary benefits of combining FoNE with other positional embedding strategies.

How does FoNE Handle numbers with longer digit sequences The maximum digit length that a float 64 data type can represent is 15 digits. When x exceeds 15 digits in length, applying FoNE(x) directly may result in a loss of precision. To address this, x can be divided into smaller chunks, and FoNE can be applied to each chunk independently. For example, x can be split into groups of five digits. The FoNE can then be calculated for each chunk, resulting in a representation of length 10 per chunk, as each digit is encoded in two dimensions. These embeddings are subsequently concatenated to obtain the final number embedding for x. Note that we are still using one token for each number. By using this method, as shown in Figure 4(b), an 8-layer transformer trained on 60-digit addition achieved an average accuracy of 97.42% across different operand length with just one forward pass. This demonstrates the effectiveness of FoNE in handling long sequences.

5 DISCUSSION

 Q1: Why not use regression loss instead of classification loss, which minimizes RMSE and can yield smaller prediction errors (Zausinger et al., 2024). The key limitation is that regression produces continuous values, making it impossible to integrate number-related tasks with general language modeling. For example, when predicting the year "1997", regression may output "1996.9999", which is acceptable under regression metrics but unusable in sequence generation or token-based reasoning. In contrast, FoNE retains a classification-based loss, so it does not require explicitly identifying which numbers are used for arithmetic. This ensures seamless compatibility with standard LLM training while still delivering accurate numerical representations.

Q2: Why does FoNE outperform other number embedding methods? Note that since FoNE uses the ratio between entries to represent numbers as shown in Lemma 3.4, it is unaffected by layer normalization and RMS normalization (Lemma D.2), in contrast to xVal (Golkar et al., 2023), which uses the magnitudes of entries. Other approaches, such as DICE (Sundararaman et al., 2020) and SALSA (Stevens et al., 2024), map numbers onto a single unit circle, which can limit their capacity to distinguish between different magnitudes effectively. FoNE, by leveraging multiple sinusoidal components, captures both the magnitude and periodicity of numbers more precisely. This comprehensive representation enables FoNE to achieve higher accuracy and generalization in number-related tasks.

Q3: Why do we choose components with periods that are multiples of 10, i.e., $10, 100, 1000 \cdots$? As shown in Zhou et al. (2024) and Figure 9, pre-trained LLMs trained on diverse datasets and strategies consistently learn nearly identical key frequency components. These components have periods of 10 and its divisors, such as 2 and 5. Since mod10 can already represent a single digit, we believe that mod 2 and mod 5 contribute to enhancing robustness. Models trained on real-world text data—where numbers are almost always expressed in decimal—commonly learn frequency components that correspond to mod10. In principle, we could choose alternative bases (such as 5, 16, etc.) to help the model better learn arithmetic in those bases, as demonstrated in Table 5. However, since most large language models primarily encounter numbers in base 10, and our results show that base-10 FoNE already performs well on arithmetic tasks in other bases (Table 4), we adopt base 10 as the default. Additional experiments validating this choice are provided in Appendix B.

Q4: Can FoNE be integrated into pretrained LLMs without harming their semantic abilities? We provide a continual pretraining experiment with a simplified version of FoNE in Appendix H, since full pretraining from scratch with LLMs is beyond the scope of this paper. The results show that FoNE can be naturally integrated into LLM pipelines: it improves arithmetic with larger numbers while preserving general language ability. This suggests that FoNE offers a practical path for enhancing numerical reasoning in existing pre-trained models without sacrificing their semantic competence. As discussed by Meng et al. (2022), the semantic associations of tokens—such as the historical or cultural meaning of a year—are often stored in the MLP layers of transformer models rather than in the token embeddings themselves. This implies that LLMs can maintain semantic knowledge of numbers in higher layers, while FoNE provides precise numerical embeddings at the input level. Consequently, the two roles are complementary: FoNE ensures accurate numerical representation, and the model's MLP layers preserve semantic meaning.

6 Conclusion

In this paper, we introduced FoNE, a novel method for representing numbers in the embedding space of LLMs. By leveraging Fourier features, FoNE directly maps numbers into a compact and precise representation, bypassing tokenization inefficiencies and preserving essential numerical properties. FoNE has significant implications for pre-training LLMs. By incorporating FoNE, models can develop a robust understanding of numerical concepts, addressing a fundamental limitation in current architectures. We believe our work establishes a solid foundation for future research on a wide range of number-related tasks, including time-series analysis, quantitative reasoning, and complex operations in fields like physics and mathematics.

REPRODUCIBILITY STATEMENT

We have taken several steps to ensure the reproducibility of our results. The FoNE method is defined step by step in Section 3.1 and Section A. Our experimental setup, including datasets, sampling rules, model configurations, and training details, is described in Section 4.1 and Appendix I.

REFERENCES

- Marah Abdin, Jyoti Aneja, Hany Awadalla, Ahmed Awadallah, Ammar Ahmad Awan, Nguyen Bach, Amit Bahree, Arash Bakhtiari, Jianmin Bao, Harkirat Behl, et al. Phi-3 technical report: A highly capable language model locally on your phone. *arXiv preprint arXiv:2404.14219*, 2024.
- Josh Achiam, Steven Adler, Sandhini Agarwal, Lama Ahmad, Ilge Akkaya, Florencia Leoni Aleman, Diogo Almeida, Janko Altenschmidt, Sam Altman, Shyamal Anadkat, et al. Gpt-4 technical report. arXiv preprint arXiv:2303.08774, 2023.
- Jiawang Bai, Li Yuan, Shu-Tao Xia, Shuicheng Yan, Zhifeng Li, and Wei Liu. Improving vision transformers by revisiting high-frequency components. In *European Conference on Computer Vision*, pp. 1–18. Springer, 2022.
- Tom B. Brown, Benjamin Mann, Nick Ryder, Melanie Subbiah, Jared Kaplan, Prafulla Dhariwal, Arvind Neelakantan, Pranav Shyam, Girish Sastry, Amanda Askell, Sandhini Agarwal, Ariel Herbert-Voss, Gretchen Krueger, Tom Henighan, Rewon Child, Aditya Ramesh, Daniel M. Ziegler, Jeffrey Wu, Clemens Winter, Christopher Hesse, Mark Chen, Eric Sigler, Mateusz Litwin, Scott Gray, Benjamin Chess, Jack Clark, Christopher Berner, Sam McCandlish, Alec Radford, Ilya Sutskever, and Dario Amodei. Language models are few-shot learners. 2020.
- Defu Cao, Furong Jia, Sercan O Arik, Tomas Pfister, Yixiang Zheng, Wen Ye, and Yan Liu. Tempo: Prompt-based generative pre-trained transformer for time series forecasting. *arXiv* preprint arXiv:2310.04948, 2023.
- Wenhu Chen, Ming Yin, Max Ku, Pan Lu, Yixin Wan, Xueguang Ma, Jianyu Xu, Xinyi Wang, and Tony Xia. Theoremqa: A theorem-driven question answering dataset. In *Proceedings of the 2023 Conference on Empirical Methods in Natural Language Processing*, pp. 7889–7901, 2023.
- Karl Cobbe, Vineet Kosaraju, Mohammad Bavarian, Mark Chen, Heewoo Jun, Lukasz Kaiser, Matthias Plappert, Jerry Tworek, Jacob Hilton, Reiichiro Nakano, et al. Training verifiers to solve math word problems. arXiv preprint arXiv:2110.14168, 2021.
- Abhimanyu Dubey, Abhinav Jauhri, Abhinav Pandey, Abhishek Kadian, Ahmad Al-Dahle, Aiesha Letman, Akhil Mathur, Alan Schelten, Amy Yang, Angela Fan, et al. The llama 3 herd of models. *arXiv preprint arXiv:2407.21783*, 2024.
- Nouha Dziri, Ximing Lu, Melanie Sclar, Xiang Lorraine Li, Liwei Jiang, Bill Yuchen Lin, Sean Welleck, Peter West, Chandra Bhagavatula, Ronan Le Bras, et al. Faith and fate: Limits of transformers on compositionality. Advances in Neural Information Processing Systems, 36, 2024.
- Xi Fang, Weijie Xu, Fiona Anting Tan, Jiani Zhang, Ziqing Hu, Yanjun Qi, Scott Nickleach, Diego Socolinsky, Srinivasan Sengamedu, and Christos Faloutsos. Large language models on tabular data–a survey. *arXiv e-prints*, pp. arXiv–2402, 2024.
- Guhao Feng, Kai Yang, Yuntian Gu, Xinyue Ai, Shengjie Luo, Jiacheng Sun, Di He, Zhenguo Li, and Liwei Wang. How numerical precision affects mathematical reasoning capabilities of llms. *arXiv preprint arXiv:2410.13857*, 2024.
- Pierre-Étienne Fiquet and Eero Simoncelli. A polar prediction model for learning to represent visual transformations. *Advances in Neural Information Processing Systems*, 36, 2024.
- Yanjun Gao, Skatje Myers, Shan Chen, Dmitriy Dligach, Timothy A Miller, Danielle Bitterman, Matthew Churpek, and Majid Afshar. When raw data prevails: Are large language model embeddings effective in numerical data representation for medical machine learning applications? *arXiv* preprint arXiv:2408.11854, 2024.

- Jonas Geiping and Tom Goldstein. Cramming: Training a language model on a single gpu in one day. In *International Conference on Machine Learning*, pp. 11117–11143. PMLR, 2023.
 - Siavash Golkar, Mariel Pettee, Michael Eickenberg, Alberto Bietti, Miles Cranmer, Geraud Krawezik, Francois Lanusse, Michael McCabe, Ruben Ohana, Liam Parker, et al. xval: A continuous number encoding for large language models. *arXiv preprint arXiv:2310.02989*, 2023.
 - Jiuxiang Gu, Chenyang Li, Yingyu Liang, Zhenmei Shi, Zhao Song, and Tianyi Zhou. Fourier circuits in neural networks: Unlocking the potential of large language models in mathematical reasoning and modular arithmetic. *arXiv* preprint arXiv:2402.09469, 2024.
 - Keji He, Chenyang Si, Zhihe Lu, Yan Huang, Liang Wang, and Xinchao Wang. Frequency-enhanced data augmentation for vision-and-language navigation. *Advances in Neural Information Processing Systems*, 36, 2024.
 - Dan Hendrycks, Collin Burns, Steven Basart, Andy Zou, Mantas Mazeika, Dawn Song, and Jacob Steinhardt. Measuring massive multitask language understanding, 2021. URL https://arxiv.org/abs/2009.03300.
 - Ermo Hua, Che Jiang, Xingtai Lv, Kaiyan Zhang, Ning Ding, Youbang Sun, Biqing Qi, Yuchen Fan, Xuekai Zhu, and Bowen Zhou. Fourier position embedding: Enhancing attention's periodic extension for length generalization. *arXiv preprint arXiv:2412.17739*, 2024.
 - Albert Q Jiang, Alexandre Sablayrolles, Arthur Mensch, Chris Bamford, Devendra Singh Chaplot, Diego de las Casas, Florian Bressand, Gianna Lengyel, Guillaume Lample, Lucile Saulnier, et al. Mistral 7b. *arXiv preprint arXiv:2310.06825*, 2023.
 - Chengyue Jiang, Zhonglin Nian, Kaihao Guo, Shanbo Chu, Yinggong Zhao, Libin Shen, and Kewei Tu. Learning numeral embeddings. *arXiv preprint arXiv:2001.00003*, 2019.
 - Ming Jin, Shiyu Wang, Lintao Ma, Zhixuan Chu, James Y Zhang, Xiaoming Shi, Pin-Yu Chen, Yux-uan Liang, Yuan-Fang Li, Shirui Pan, et al. Time-llm: Time series forecasting by reprogramming large language models. *arXiv preprint arXiv:2310.01728*, 2023.
 - Zhijing Jin, Yuen Chen, Felix Leeb, Luigi Gresele, Ojasv Kamal, Zhiheng Lyu, Kevin Blin, Fernando Gonzalez Adauto, Max Kleiman-Weiner, Mrinmaya Sachan, et al. Cladder: A benchmark to assess causal reasoning capabilities of language models. *Advances in Neural Information Processing Systems*, 36, 2024.
 - Subhash Kantamneni and Max Tegmark. Language models use trigonometry to do addition. *arXiv* preprint arXiv:2502.00873, 2025.
 - Nayoung Lee, Kartik Sreenivasan, Jason D Lee, Kangwook Lee, and Dimitris Papailiopoulos. Teaching arithmetic to small transformers. *arXiv preprint arXiv:2307.03381*, 2023.
 - Amit Arnold Levy and Mor Geva. Language models encode numbers using digit representations in base 10. *arXiv preprint arXiv:2410.11781*, 2024.
 - Shixuan Li, Wei Yang, Peiyu Zhang, Xiongye Xiao, Defu Cao, Yuehan Qin, Xiaole Zhang, Yue Zhao, and Paul Bogdan. Climatellm: Efficient weather forecasting via frequency-aware large language models. *arXiv preprint arXiv:2502.11059*, 2025.
 - Jack Lindsey, Wes Gurnee, Emmanuel Ameisen, Brian Chen, Adam Pearce, Nicholas L. Turner, Craig Citro, David Abrahams, Shan Carter, Basil Hosmer, Jonathan Marcus, Michael Sklar, Adly Templeton, Trenton Bricken, Callum McDougall, Hoagy Cunningham, Thomas Henighan, Adam Jermyn, Andy Jones, Andrew Persic, Zhenyi Qi, T. Ben Thompson, Sam Zimmerman, Kelley Rivoire, Thomas Conerly, Chris Olah, and Joshua Batson. On the biology of a large language model. *Transformer Circuits Thread*, 2025. URL https://transformer-circuits.pub/2025/attribution-graphs/biology.html#dives-addition.
 - Peiyuan Liu, Hang Guo, Tao Dai, Naiqi Li, Jigang Bao, Xudong Ren, Yong Jiang, and Shu-Tao Xia. Taming pre-trained llms for generalised time series forecasting via cross-modal knowledge distillation. *arXiv preprint arXiv:2403.07300*, 2024a.

- Xiao Liu, Zirui Wu, Xueqing Wu, Pan Lu, Kai-Wei Chang, and Yansong Feng. Are Ilms capable of data-based statistical and causal reasoning? benchmarking advanced quantitative reasoning with data. *arXiv preprint arXiv:2402.17644*, 2024b.
 - Qianli Ma, Zhen Liu, Zhenjing Zheng, Ziyang Huang, Siying Zhu, Zhongzhong Yu, and James T Kwok. A survey on time-series pre-trained models. *IEEE Transactions on Knowledge and Data Engineering*, 2024.
 - Sean McLeish, Arpit Bansal, Alex Stein, Neel Jain, John Kirchenbauer, Brian R Bartoldson, Bhavya Kailkhura, Abhinav Bhatele, Jonas Geiping, Avi Schwarzschild, et al. Transformers can do arithmetic with the right embeddings. *arXiv preprint arXiv:2405.17399*, 2024a.
 - Sean McLeish, Avi Schwarzschild, and Tom Goldstein. Benchmarking chatgpt on algorithmic reasoning. *arXiv preprint arXiv:2404.03441*, 2024b.
 - Kazem Meidani, Parshin Shojaee, Chandan K Reddy, and Amir Barati Farimani. Snip: Bridging mathematical symbolic and numeric realms with unified pre-training. *arXiv preprint arXiv:2310.02227*, 2023.
 - Kevin Meng, David Bau, Alex Andonian, and Yonatan Belinkov. Locating and editing factual associations in gpt. *Advances in Neural Information Processing Systems*, 35:17359–17372, 2022.
 - Neel Nanda, Lawrence Chan, Tom Lieberum, Jess Smith, and Jacob Steinhardt. Progress measures for grokking via mechanistic interpretability. *arXiv preprint arXiv:2301.05217*, 2023.
 - Rodrigo Nogueira, Zhiying Jiang, and Jimmy Lin. Investigating the limitations of transformers with simple arithmetic tasks. *arXiv preprint arXiv:2102.13019*, 2021.
 - Maxwell Nye, Anders Johan Andreassen, Guy Gur-Ari, Henryk Michalewski, Jacob Austin, David Bieber, David Dohan, Aitor Lewkowycz, Maarten Bosma, David Luan, et al. Show your work: Scratchpads for intermediate computation with language models. *arXiv preprint arXiv:2112.00114*, 2021.
 - Chris Olah, Nick Cammarata, Ludwig Schubert, Gabriel Goh, Michael Petrov, and Shan Carter. An overview of early vision in inceptionv1. *Distill*, 5(4):e00024–002, 2020.
 - Bruno A Olshausen and David J Field. Sparse coding with an overcomplete basis set: A strategy employed by v1? *Vision research*, 37(23):3311–3325, 1997.
 - Panupong Pasupat and Percy Liang. Compositional semantic parsing on semi-structured tables. In *Proceedings of the 53rd Annual Meeting of the Association for Computational Linguistics and the 7th International Joint Conference on Natural Language Processing (Volume 1: Long Papers)*, pp. 1470–1480, Beijing, China, July 2015. Association for Computational Linguistics. doi: 10.3115/v1/P15-1142. URL https://aclanthology.org/P15-1142.
 - Yasaman Razeghi, Robert L Logan IV, Matt Gardner, and Sameer Singh. Impact of pretraining term frequencies on few-shot reasoning. *arXiv* preprint arXiv:2202.07206, 2022.
 - Maria Sahakyan, Zeyar Aung, and Talal Rahwan. Explainable artificial intelligence for tabular data: A survey. *IEEE access*, 9:135392–135422, 2021.
 - David Saxton, Edward Grefenstette, Felix Hill, and Pushmeet Kohli. Analysing mathematical reasoning abilities of neural models. *arXiv* preprint arXiv:1904.01557, 2019.
 - Jiandong Shao, Yao Lu, and Jianfei Yang. Benford's curse: Tracing digit bias to numerical hallucination in llms. *arXiv preprint arXiv:2506.01734*, 2025.
 - Ruoqi Shen, Sébastien Bubeck, Ronen Eldan, Yin Tat Lee, Yuanzhi Li, and Yi Zhang. Positional description matters for transformers arithmetic. *arXiv preprint arXiv:2311.14737*, 2023.
 - Safal Shrestha, Minwu Kim, and Keith Ross. Mathematical reasoning in large language models: Assessing logical and arithmetic errors across wide numerical ranges. *arXiv preprint arXiv:2502.08680*, 2025.

- Jasivan Alex Sivakumar and Nafise Sadat Moosavi. How to leverage digit embeddings to represent numbers? *arXiv preprint arXiv:2407.00894*, 2024.
 - Samuel Stevens, Emily Wenger, Cathy Li, Niklas Nolte, Eshika Saxena, François Charton, and Kristin Lauter. Salsa fresca: angular embeddings and pre-training for ml attacks on learning with errors. *arXiv preprint arXiv:2402.01082*, 2024.
 - Dhanasekar Sundararaman, Shijing Si, Vivek Subramanian, Guoyin Wang, Devamanyu Hazarika, and Lawrence Carin. Methods for numeracy-preserving word embeddings. In *Proceedings of the 2020 Conference on Empirical Methods in Natural Language Processing (EMNLP)*, pp. 4742–4753, 2020.
 - Mingtian Tan, Mike A Merrill, Vinayak Gupta, Tim Althoff, and Thomas Hartvigsen. Are language models actually useful for time series forecasting? *arXiv preprint arXiv:2406.16964*, 2024.
 - Matthew Tancik, Pratul Srinivasan, Ben Mildenhall, Sara Fridovich-Keil, Nithin Raghavan, Utkarsh Singhal, Ravi Ramamoorthi, Jonathan Barron, and Ren Ng. Fourier features let networks learn high frequency functions in low dimensional domains. *Advances in neural information processing systems*, 33:7537–7547, 2020.
 - Avijit Thawani, Jay Pujara, Pedro A Szekely, and Filip Ilievski. Representing numbers in nlp: a survey and a vision. *arXiv preprint arXiv:2103.13136*, 2021.
 - Hugo Touvron, Louis Martin, Kevin Stone, Peter Albert, Amjad Almahairi, Yasmine Babaei, Nikolay Bashlykov, Soumya Batra, Prajjwal Bhargava, Shruti Bhosale, et al. Llama 2: Open foundation and fine-tuned chat models. *arXiv preprint arXiv:2307.09288*, 2023.
 - Ashish Vaswani, Noam Shazeer, Niki Parmar, Jakob Uszkoreit, Llion Jones, Aidan N Gomez, Łukasz Kaiser, and Illia Polosukhin. Attention is all you need. *Advances in neural information processing systems*, 30, 2017.
 - Jason Wei, Xuezhi Wang, Dale Schuurmans, Maarten Bosma, Fei Xia, Ed Chi, Quoc V Le, Denny Zhou, et al. Chain-of-thought prompting elicits reasoning in large language models. *Advances in neural information processing systems*, 35:24824–24837, 2022.
 - Longhui Yu, Weisen Jiang, Han Shi, Jincheng Yu, Zhengying Liu, Yu Zhang, James T Kwok, Zhenguo Li, Adrian Weller, and Weiyang Liu. Metamath: Bootstrap your own mathematical questions for large language models. *arXiv preprint arXiv:2309.12284*, 2023.
 - Jonas Zausinger, Lars Pennig, Anamarija Kozina, Sean Sdahl, Julian Sikora, Adrian Dendorfer, Timofey Kuznetsov, Mohamad Hagog, Nina Wiedemann, Kacper Chlodny, et al. Regress, don't guess–a regression-like loss on number tokens for language models. *arXiv preprint arXiv:2411.02083*, 2024.
 - Fan Zhou, Zengzhi Wang, Nikhil Ranjan, Zhoujun Cheng, Liping Tang, Guowei He, Zhengzhong Liu, and Eric P. Xing. Megamath: Pushing the limits of open math corpora, 2025. URL https://arxiv.org/abs/2504.02807.
 - Hattie Zhou, Arwen Bradley, Etai Littwin, Noam Razin, Omid Saremi, Josh Susskind, Samy Bengio, and Preetum Nakkiran. What algorithms can transformers learn? a study in length generalization. *arXiv preprint arXiv:2310.16028*, 2023a.
 - Tian Zhou, Peisong Niu, Liang Sun, Rong Jin, et al. One fits all: Power general time series analysis by pretrained lm. *Advances in neural information processing systems*, 36:43322–43355, 2023b.
 - Tianyi Zhou, Deqing Fu, Vatsal Sharan, and Robin Jia. Pre-trained large language models use fourier features to compute addition. *arXiv preprint arXiv:2406.03445*, 2024.

APPENDIX A Detailed Algorithms for Computing FoNE, and Making Predictions B FoNE on Binary Classification and Modular Arithmetic Task C More Related Work **D** Preliminaries and Missing Proofs **E** More Evidence F FoNE for 60-digit Integer Addition in One Forward Pass **G** Combining FoNE with Abacus **H** Continue Pretraining LLMs with Simplified FoNE I More Details on Experimental Setup J Replicating Results on GPT2-Large Based Model **K** R^2 Comparison for Different Arithmetic Tasks

A DETAILED ALGORITHMS FOR COMPUTING FONE, AND MAKING PREDICTIONS

In this section, we provide the detail pipeline and algorithms of how we compute FoNE, get the final loss and final prediction as defined in Section 3.1.

We first show the how are FoNE and Fourier number decoding integrated with regular Transformer pipeline.

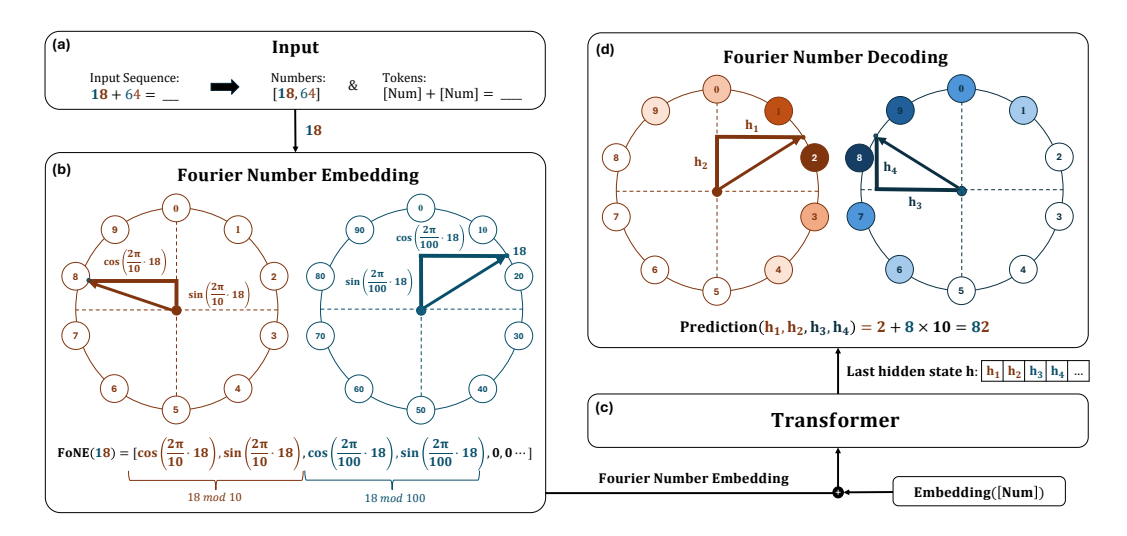


Figure 5: (a) We extract all the numbers from the input sequence. (b) For each number, we use FoNE to directly map the number to its embedding. The first two entries in the embedding represent $18 \mod 10$, while the next two entries represent $18 \mod 100$. (c) We pad the FoNE with zeros, add it to the word embeddings, and then feed the combined embeddings into the model. (d) For each digit, we take every two entries from the last hidden state and find the number whose representation is closest to these two entries.

Next we show the exact algorithms we use to compute FoNE, compute loss and make the final prediction.

Algorithm 1 Fourier Number Embedding (FoNE) Algorithm

```
1: procedure FOURIERNUMBEREMBEDDING(x \in \mathbb{R}, m \in \mathbb{Z}_{>0}, n \in \mathbb{Z}_{>0}, d \in \mathbb{Z}_{>0})
        Inputs: Number x, integer digit length m, decimal digit length n, embedding dimension d
 3:
        Initialize empty embedding vector FoNE \leftarrow []
        for i = -n+1 \rightarrow m do
                                                                \triangleright Loop over all scales from 10^{-n+1} to 10^m
 4:
                                                                        ⊳ Set the period for the current scale
 5:
             T_i \leftarrow 10^i
             \phi(x, T_i) \leftarrow (\cos(\frac{2\pi}{T_i}x), \sin(\frac{2\pi}{T_i}x))
                                                            \triangleright Compute the circular embedding for scale T_i
 6:
 7:
             Append \phi(x, T_i) to FoNE
                                                           ▷ Add the embedding for this scale to the result
 8:
        end for
 9:
        while Length(FoNE) < d do
                                                       ▶ Ensure embedding dimension matches the target
10:
             Append 0 to FoNE
                                                                                                     end while
11:
        return FoNE
12:
13: end procedure
```

Algorithm 2 Fourier Number Loss & Prediction

810

811

812

813

814

815

816

817

818

819

820 821

822

823 824 825

826

827

828

829

830

831

832

833

834

835

836

837

838

839

840

841

842

843

844

845

846

847

848

849

850

851852853

854 855

856

857 858

859

860

861

862

863

```
1: function FOURIERNUMBERLOSSFUNCTION(h, y, i)
          y_i \leftarrow \text{the } i\text{-th digit of } y
          a \leftarrow |h[2i], h[2i+1]|
          b \leftarrow [\phi(0,10), \phi(1,10), \cdots, \phi(9,10)]^{\top}
 4:
 5:
          logits \leftarrow a \cdot b
          loss \leftarrow L_{CE}(y_i, logits)
 6:
                                                                                               \triangleright Cross-entropy loss for digit i
 7:
          return loss
 8: end function
 9: function FOURIERNUMBERPREDICTION(h, i)
                                                                                                          \triangleright Prediction for digit i
          logits \leftarrow [h[2i], h[2i+1]] \cdot [\phi(j, 10)]_{j=0,\dots,9}
10:
11:
          \widehat{y}_i \leftarrow \arg\max_{j \in \{0,\dots,9\}} \operatorname{logits}[j]
12:
          return \hat{y}_i
13: end function
```

Algorithm 3 Fourier Number Final Loss & Prediction

```
1: function FOURIERNUMBERFINALLOSS(h, y, m, n)

    Compute average loss

           totalLoss \leftarrow 0
 3:
           \mathcal{I} \leftarrow [m+n]
 4:
           for i \in \mathcal{I} do
 5:
                 digitLoss \leftarrow FourierNumberLossFunction(h, y, i)
 6:
                 totalLoss \leftarrow totalLoss + digitLoss
           end for
 7:
           finalLoss \leftarrow \tfrac{totalLoss}{^{_{|\mathcal{T}|}}}
 8:
                                                                                                 > Average over all digit positions
 9:
           return finalLoss
10: end function
11: function FOURIERNUMBERFINALPREDICTION(h, m, n)
                                                                                                          ⊳ Compute final prediction
12:
           \widehat{y} \leftarrow 0
13:
           \mathcal{I}_{\text{frac}} \leftarrow [0, \dots, n-1]
                                                                                                             > Fractional digit indices
           \mathcal{I}_{\text{int}} \leftarrow [n, \dots, m+n-1]
                                                                                                                 14:
           for i \in \mathcal{I}_{frac} do
15:
                logits_i \leftarrow [h[2i], h[2i+1]] \cdot [\phi(j, 10)]_{i=0,\dots,9}
16:
17:
                \widehat{y}_i \leftarrow \arg\max_{j \in \{0,\dots,9\}} \operatorname{logits}_i[j]
18:
                \widehat{y} \leftarrow \widehat{y} + \widehat{y}_i \cdot 10^{-(n-i)}
                                                                                              \triangleright Scale fractional part by 10^{-(n-i)}
19:
           end for
20:
           for j \in \mathcal{I}_{int} do
                logits_i \leftarrow [h[2j], h[2j+1]] \cdot [\phi(j,10)]_{i=0,\dots,9}
21:
                \widehat{y}_j \leftarrow \arg\max_{j \in \{0, \dots, 9\}} \operatorname{logits}_j[j]
22:
                \widehat{y} \leftarrow \widehat{y} + \widehat{y}_j \cdot 10^{j-n}
23:
                                                                                                          \triangleright Scale integer part by 10^{j}
24:
           end for
25:
           return \hat{y}
26: end function
```

B FONE ON BINARY CLASSIFICATION AND MODULAR ARITHMETIC TASK

In this section, we demonstrate that FoNE outperforms other methods on binary classification tasks and modular arithmetic tasks, benefiting from its precise representation.

Binary Classification Task Each example in the dataset is formatted as [num1, num2, num3], where the integers num1, num2, and num3 are sorted in ascending order ($num1 \le num2 \le num3$) to ensure uniqueness and eliminate duplicate representations of the same combination. The integers are uniformly sampled from the range [0,1000]. The label for each example is determined by evaluating the linear equation

```
a \cdot \text{num1} + b \cdot \text{num2} + c \cdot \text{num3} - d,
```

using predefined coefficients a=1.5, b=-2, c=0.5, and d=10 and a=1.5, b=-2, c=0.5, and d=-190. If the result is greater than zero, the label is assigned as 1; otherwise, it is assigned as 0. The dataset is divided into training, validation, and test subsets, as outlined in Table 9. Figure 6 and Figure 7 show that FoNE outperforms the regular embedding method, XVAL, and even a fine-tuned Llama-3.2-1B model by requiring less data and achieving higher accuracy.

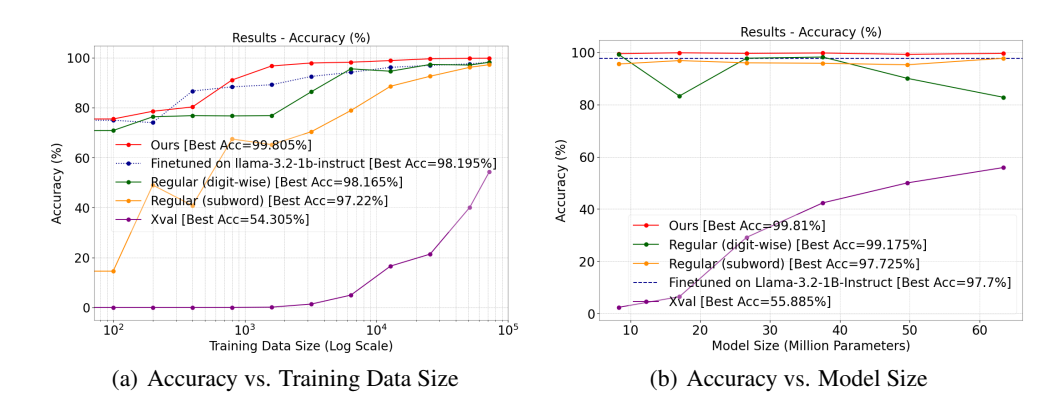


Figure 6: We train Llama-3.2-1B from scratch with random initialization using different number embedding methods on number classification where d=10. The test accuracy is compared across varying data sizes and model sizes.

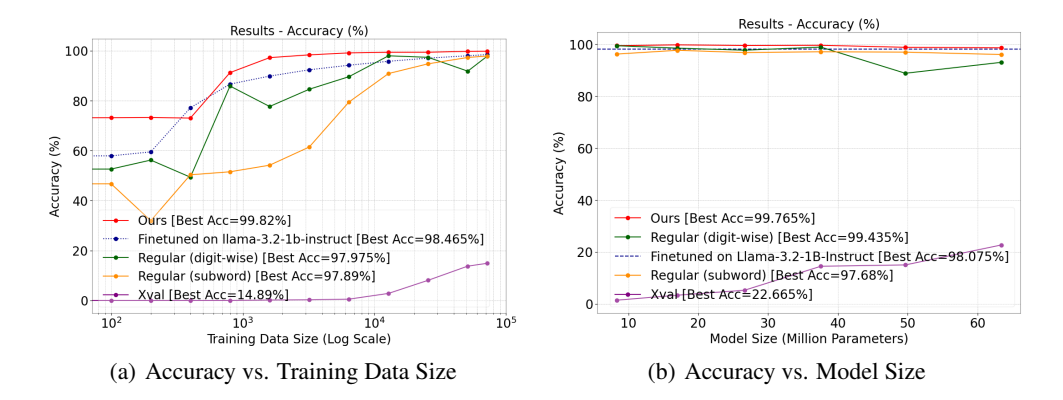


Figure 7: We train Llama-3.2-1B from scratch with random initialization using different number embedding methods on number classification where d=-190. The test accuracy is compared across varying data sizes and model sizes.

Modular Arithmetic and Base Selection We conduct experiments varying the FoNE base from 7 to 13 and observed a clear "sweet spot" at base 10. For example, at base 7 the addition, subtraction, and multiplication accuracies are only 17.66 %, 1.93 %, and 0.54 %, respectively, while at base 10 we achieve 100 % accuracy on addition and subtraction after just 4 and 26 epochs, and 99.25 % on multiplication after 50 epochs. Accuracy then fall off again at larger bases (e.g., at base 13: 1.06 %, 5.71 %, and 1.91 %). This confirms that bases that are too small or too large degrade digit-level distinguishability.

We also aligned FoNE's moduli to the numbers' representation base by preprocessing inputs into base 5. In that setting, only the FoNE embedding with period 5 reached perfect accuracy (100 % in 6 epochs), whereas other periods (2–4 and 7–8) yielded near-zero to sub-20 % accuracy (e.g., period 2: 0.25 %; period 3: 0.12 %; period 7: 16.38 %). This again demonstrates that FoNE performs best when its moduli match the underlying digit base.

Table 4: Accuracy (%) on arithmetic tasks under different bases.

Base	Epochs (Add/Sub/Mul)	Accuracy (Add/Sub/Mul)
7	50 / 50 / 50	17.66 / 1.93 / 0.54
8	50 / 50 / 50	40.91 / 6.07 / 0.33
9	50 / 50 / 50	65.49 / 65.63 / 65.78
10	4/26/50	100.00 / 100.00 / 99.25
11	50 / 50 / 50	99.99 / 99.99 / 78.76
12	50 / 50 / 50	99.78 / 99.99 / 54.14
13	50 / 50 / 50	1.06 / 5.71 / 1.91

Table 5: Accuracy (%) with base-5 number inputs, under varying FoNE periods.

FoNE Period	Epochs	Accuracy (%)
2	50	0.25
3	50	0.12
4	50	0.17
5	6	100.00
7	50	16.38
8	50	99.97

We additionally benchmarked FoNE on modular addition tasks with varying moduli. The goal is to predict $x+y \mod m$, where $x,y \in [0,m)$. FoNE consistently outperforms standard tokenization, especially at higher moduli.

Table 6: Accuracy (%) on modular addition tasks across various moduli.

$\mathbf{Modulus}\ m$	FoNE Accuracy	Standard Tokenization Accuracy
11	100.00	99.98
60	99.27	99.99
97	100.00	0.89
100	100.00	18.17
113	100.00	99.99
121	100.00	5.48
225	100.00	65.10
256	100.00	70.20
257	100.00	11.36

These experiments validate our claim that FoNE is most effective when its moduli align with the target numeral base, and it remains robust even in high-modulus arithmetic settings where standard tokenization breaks down.

C MORE RELATED WORK

Fourier Features. Fourier features are commonly observed in image models, particularly in the early layers of vision models Olshausen & Field (1997); Olah et al. (2020); Fiquet & Simoncelli (2024). These features enable the model to detect edges, textures, and other spatial patterns effectively. However, Transformers struggle to capture high-frequency components (Bai et al., 2022; Tancik et al., 2020). Augmenting data with high-frequency components or explicitly encoding coordinates using Fourier features has been demonstrated to improve model performance (Tancik et al., 2020; He et al., 2024; Hua et al., 2024). In fact, the original Transformers paper (Vaswani et al., 2017) uses Fourier features to encode the position information of tokens; however, it does not apply this idea to number tokens to aid with numerical tasks. In modular addition tasks, studies have revealed that after "grokking," a one-layer Transformer can learn to solve the task perfectly by leveraging Fourier features (Nanda et al., 2023; Gu et al., 2024). Furthermore, Zhou et al. (2024) demonstrate that LLMs naturally encode numbers using Fourier features during pretraining, leveraging these representations for arithmetic tasks (Levy & Geva, 2024; Kantamneni & Tegmark, 2025; Lindsey

et al., 2025). Building on this insight, we propose using modular Fourier components to explicitly represent digits, enabling models to perform precise numerical computation. This allows algebraic operations to be carried out in a component-wise, parallel manner and overcomes the limitations of token-based number representations.

D PRELIMINARIES AND MISSING PROOFS

D.1 PRELIMINARIES

In this section, we provide the necessary mathematical definitions and concepts used throughout the paper.

Period and Frequency. A function f(x) is periodic with period T>0 if f(x+T)=f(x) for all x. The period T represents the smallest positive value for which the function repeats. The frequency f of a periodic function is the reciprocal of its period, $f=\frac{1}{T}$, and describes the number of cycles completed in one unit interval. For the sine and cosine functions $\cos\left(\frac{2\pi}{T}x\right)$ and $\sin\left(\frac{2\pi}{T}x\right)$, the period is T.

Unit Circle. The unit circle is the set of points in the plane at a distance of 1 from the origin, given by $x^2 + y^2 = 1$. The coordinates of points on the unit circle can be parameterized as $(\cos \theta, \sin \theta)$, where θ is the angle measured counterclockwise from the positive x-axis. For any angle θ , $\cos \theta$ represents the x-coordinate, and $\sin \theta$ represents the y-coordinate.

Two-Argument Inverse Tangent. The two-argument inverse tangent function, atan2(y, x), determines the angle θ (modulo 2π) given the coordinates $(x, y) = (\cos \theta, \sin \theta)$. Specifically,

$$\theta = \operatorname{atan2}(y, x),$$

which resolves the angle θ uniquely based on the signs of x and y.

Modular Arithmetic. Modular arithmetic considers equivalence classes of numbers under a modulus T > 0. For integers a and b, $a \equiv b \pmod{T}$ if $T \mid (a - b)$, meaning a and b differ by an integer multiple of T.

Fourier Representation. Periodic functions with period T can be represented using the fundamental frequencies $\frac{2\pi}{T}$. For example, the embeddings $\left(\cos\left(\frac{2\pi}{T}x\right),\sin\left(\frac{2\pi}{T}x\right)\right)$ capture the periodicity of x modulo T by mapping it to a unique point on the unit circle.

D.2 MISSING PROOFS

In this section, we provide some missing proofs.

Lemma D.1 (Formal version of Lemma 3.3). Given the pair $\left(\cos\left(\frac{2\pi}{T}x\right), \sin\left(\frac{2\pi}{T}x\right)\right)$, we can recover $x \mod T$.

Proof. Let $\theta = \frac{2\pi}{T} x$. Then the given pair becomes

$$(\cos(\theta), \sin(\theta)).$$

From this pair, one can recover θ uniquely modulo 2π . Concretely, θ can be obtained (modulo 2π) using the two-argument inverse tangent function:

$$\theta \equiv \operatorname{atan2}(\sin(\theta), \cos(\theta)) \pmod{2\pi}.$$

Since $\theta = \frac{2\pi}{T} x$, we have

$$x = \frac{T}{2\pi} \theta.$$

Hence x is determined up to integer multiples of T, i.e., $x \mod T$.

1025 In other words, if

$$\left(\cos(\tfrac{2\pi}{T}x_1),\sin(\tfrac{2\pi}{T}x_1)\right) \; = \; \left(\cos(\tfrac{2\pi}{T}x_2),\sin(\tfrac{2\pi}{T}x_2)\right),$$

then $\frac{2\pi}{T}x_1 \equiv \frac{2\pi}{T}x_2 \pmod{2\pi}$, which implies $x_1 \equiv x_2 \pmod{T}$. Therefore, from the pair $\left(\cos(\frac{2\pi}{T}x),\sin(\frac{2\pi}{T}x)\right)$, we can indeed recover $x \bmod T$.

Lemma D.2 (Layer-Normalized FoNE Preserves Numeracy). Given a number's Layer-Normalized Fourier Number Embedding $LN(FoNE(x) + \mathbf{p})$, where FoNE(x) is the Fourier Number Embedding of x and \mathbf{p} is an orthogonal positional encoding vector, assume the mean of $FoNE(x) + \mathbf{p}$ is 0. Let m be the integer digit length of x and n be the decimal digit length of x. Then, using Lemma 3.3, we can recover $x \mod 10^i$ for each integer i in the range -n+1 to m.

Proof. Assume the mean of $\mathbf{x} = \mathsf{FoNE}(x) + \mathbf{p}$ is 0, i.e., $\mu = 0$. Under this assumption, LayerNorm simplifies to:

$$LN(\mathbf{x}) = \frac{\mathbf{x}}{\sigma},$$

where σ is the standard deviation of x.

Let $\mathbf{u} = \mathsf{FoNE}(x)$ encode the scalar x, and let \mathbf{p} be an orthogonal positional encoding vector such that:

$$\|\mathbf{u}\| = \|\mathbf{p}\| = 1$$
 and $\mathbf{u} \cdot \mathbf{p} = 0$.

Then, the input to LayerNorm is:

$$x = u + p$$
.

The standard deviation σ of x is given by:

$$\sigma = \sqrt{\frac{1}{d} \sum_{i=1}^{d} (\mathbf{x}_i - \mu)^2},$$

where d is the dimensionality of x. Since $\mu = 0$, this simplifies to:

$$\sigma = \sqrt{\frac{1}{d} \|\mathbf{x}\|^2}.$$

Substitute x = u + p:

$$\|\mathbf{x}\|^2 = \|\mathbf{u} + \mathbf{p}\|^2 = \|\mathbf{u}\|^2 + \|\mathbf{p}\|^2 + 2\mathbf{u} \cdot \mathbf{p}.$$

By orthogonality and unit norm, $\mathbf{u} \cdot \mathbf{p} = 0$, $\|\mathbf{u}\|^2 = 1$, and $\|\mathbf{p}\|^2 = 1$. Thus:

$$\|\mathbf{x}\|^2 = 1 + 1 + 0 = 2.$$

Therefore:

$$\sigma = \sqrt{\frac{1}{d} \cdot 2} = \sqrt{\frac{2}{d}}.$$

The LayerNorm operation simplifies to:

$$LN(\mathbf{x}) = \frac{\mathbf{x}}{\sigma} = \frac{\mathbf{u} + \mathbf{p}}{\sqrt{\frac{2}{d}}} = \sqrt{\frac{d}{2}}(\mathbf{u} + \mathbf{p}).$$

This rescales **u** and **p** by a factor of $\sqrt{\frac{d}{2}}$.

The key observation is that LayerNorm applies a **uniform scaling** to all components of \mathbf{x} . Since \mathbf{u} and \mathbf{p} are orthogonal and their relative directions are preserved, the numerical relationships encoded in \mathbf{u} (which represent x) are preserved up to a scaling factor.

By Lemma 3.3, the numeracy of x is preserved. This means we can recover $x \mod 10^i$ for all i in the range $-n+1 \le i \le m$, as the normalized embedding retains the necessary information about x.

The same result holds for RMSNorm because it also applies a uniform scaling (based on the root mean square of the input) while preserving the relative directions of the embedding components, thus maintaining the numeracy of x.

Notet that standard sinusoidal positional encodings (PEs) (Vaswani et al., 2017) cannot serve as a substitute for numerical embeddings. PEs are explicitly constructed to distinguish token positions in a sequence, not to represent the magnitude or digit structure of real numbers. They use a fixed set of exponentially spaced frequencies to ensure each position has a unique yet non-invertible signature; as a result, there is no straightforward way to recover the original numeric value (or its individual digits) from a PE embedding. Moreover, the frequencies in PEs are chosen for positional uniqueness, not for digit-aligned modular arithmetic, so small changes in numeric value can produce large, non-monotonic changes in the embedding space—precisely the opposite of the smooth, digit-wise variation required for accurate number encoding. Unlike FNE's digit-aligned sinusoidal components (e.g., mod 10, mod 100, ...), PEs do not guarantee invertibility with respect to numeric operations.

E MORE EVIDENCE

E.1 LLMs Struggle with Multi-digit Arithmetic

We evaluate five production LLMs (Claude 3.7 Sonnet, DeepSeek V3.1, Gemini 2.5 Flash, GPT-5, and Qwen3-235B) on direct arithmetic without chain-of-thought, code execution, or tools. For each setting, we sample 100 IID problem instances with uniformly distributed operands over the full d-digit numbers. Tasks include $d \in \{3,4,5,6\}$ for multiplication and $d \in \{7,8,50\}$ for addition. Models receive a two-shot, operation-matched prompt and must return a single integer only. Decoding uses temperature 0. We parse the first integer token from the response and score exact-match accuracy by numeric equality with the reference.

		Multiplication				Additio	n
Model	3	4	5	6	7	8	50
Claude 3.7 Sonnet DeepSeek V3.1 Gemini 2.5 Flash GPT-5 Qwen3-235B	1.00 0.94 0.58 0.74 0.94	0.53 0.25 0.11 0.09 0.62	0.02 0.01 0.00 0.00 0.05	0.00 0.00 0.00 0.00 0.00	1.00 0.95 0.99 0.98 0.99	0.97 0.95 0.96 0.92 0.98	0.82 0.34 0.33 0.66 0.28

Table 7: Exact-match accuracy on direct multi-digit arithmetic; columns indicate digits per operand. Each entry averages 100 IID problems per setting with uniformly sampled d-digit operands. Two-shot prompting, single-integer output only.

Results. Even the most recently released LLMs still struggle with *multi-digit multiplication*, while fail to achieve perfect accuracy on *addition*. For multiplication, accuracy drops sharply as operand length increases: models perform well on 3-digit multiplication (≥ 0.58), but fall below 0.10 for 5-digit cases and nearly 0 at 6 digits. Qwen3-235B is the most robust, reaching 0.62 on 4-digit and 0.05 on 5-digit multiplication, yet still fails on 6 digits. For addition, all models achieve ≥ 0.95 on 7–8 digit tasks, but accuracy declines on long-sequence addition (50 digits), ranging from 0.28 (Qwen3-235B) to 0.82 (Claude 3.7 Sonnet). In summary, LLMs excel at addition with short to medium operands but remain brittle for both long-sequence addition and especially large-digit multiplication.

E.2 EMERGENCE OF FOURIER FEATURES DURING PRE-TRAINING

We follow Zhou et al. (2024) and conduct the same Fourier analysis on Pythia model. In Figure 8, we show how Pythia gradually learns the Fourier features during pre-training. With different model size, the model gradually learn the same frequency components.

We extend the work of Zhou et al. (2024) to other pre-trained LLMs and observe similar findings: pre-trained LLMs, regardless of the dataset used, tend to learn the same outlier frequency components.

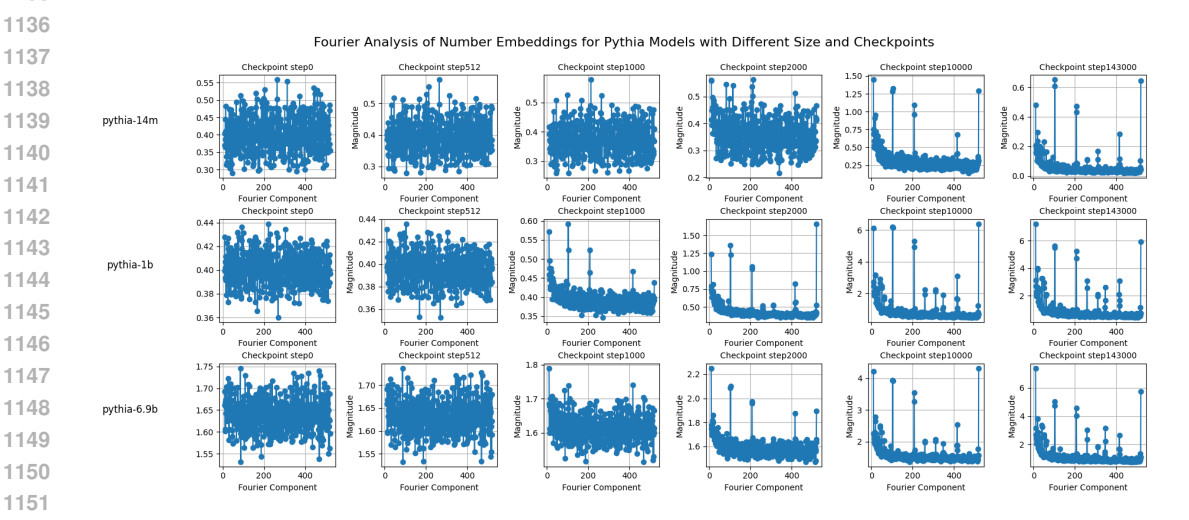


Figure 8: Fourier analysis of the Pythia model's number embeddings across pre-training checkpoints. The figure illustrates how the Fourier features are progressively learned during pre-training, showing the emergence of specific frequency components. Models of varying sizes exhibit a similar trend, gradually learning the same frequency components over time.

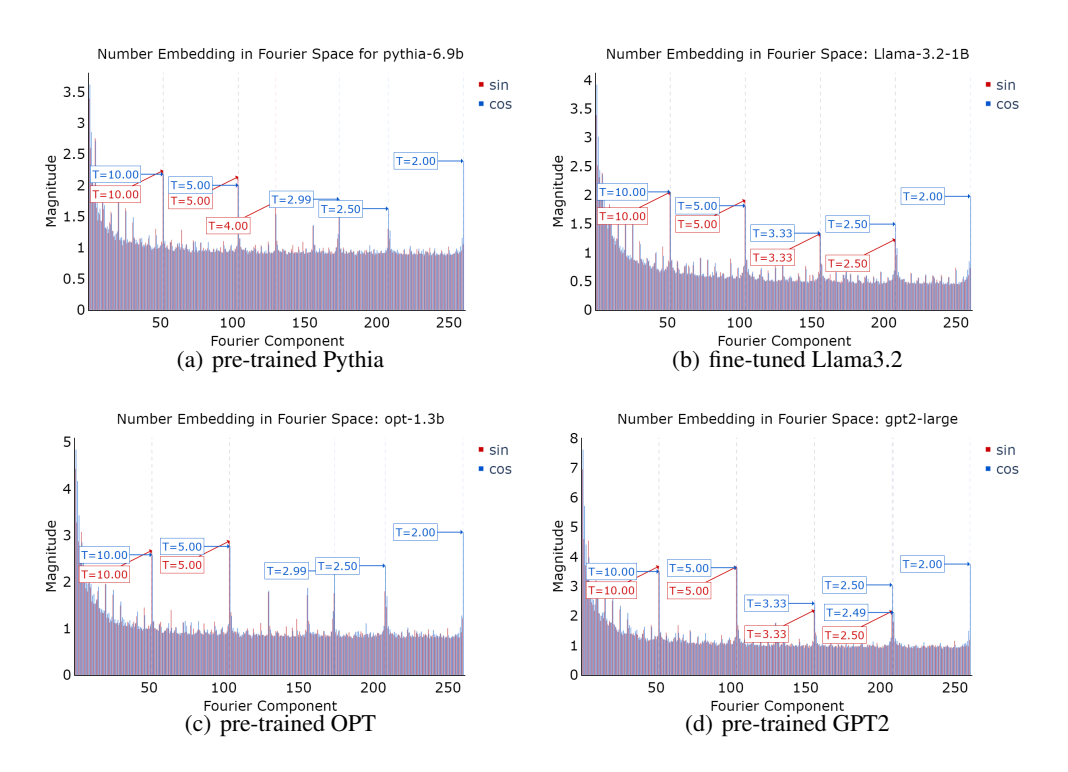


Figure 9: Number embedding in Fourier space for different pre-trained models.

F FONE FOR 60-DIGIT INTEGER ADDITION IN ONE FORWARD PASS

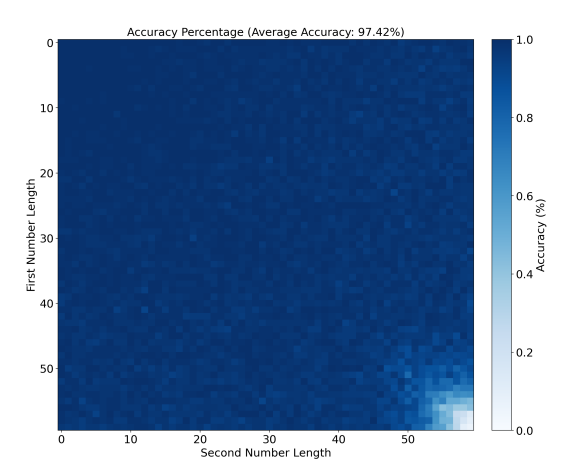


Figure 10: Accuracy of an 8-layer transformer on 60-digit addition tasks, illustrating the effectiveness of FoNE embeddings in handling long sequences. The model achieves an average accuracy of 97.42% across different operand lengths, showcasing its capability in numerical precision and sequence representation.

As discussed in Section 5, the maximum digit length that a float 64 data type can precisely represent is 15 digits. Consequently, even if we convert numbers to float 64 and then back to float 16 to match the model weight precisionm it still introduce numerical inaccuracies when the input x exceeds 15 digits. To mitigate this issue, we process x by dividing it into smaller chunks, allowing the FoNE to operate effectively without precision loss.

Specifically, x is split into groups of five digits, and FoNE is applied independently to each chunk. Each digit within a chunk is encoded into two dimensions, resulting in an embedding of length 10 per chunk. These chunk embeddings are then concatenated to form the final representation of x. This method ensures that even for long inputs, the FoNE still preserve the numeracy of the numbers.

We adopt the data generation approach from McLeish et al. (2024a), which includes all combinations of operand lengths (i,j) up to a maximum length k, generating 20 million stratified samples to ensure balanced representation across all length pairs. Training is conducted using a language model cramming approach (Geiping & Goldstein, 2023), constrained to 8 exaFLOP (equivalent to 24 hours of training on a single Nvidia RTX A6000 GPU). Using this strategy, as depicted in Figure 4(a), an 8-layer transformer trained on 60-digit addition achieves an average accuracy of 97.42% across various operand lengths in just one forward pass. This result underscores the effectiveness of the FoNE in processing long numbers with high precision and computational efficiency in just one forward pass.

G COMBINING FONE WITH ABACUS

We train decoder-only causal language models to solve arithmetic problems, following the setup described in McLeish et al. (2024a). Inputs are formatted in a least-significant-digit-first order (e.g., 98282 + 3859172 = 2787472), without padding between digits or operands. The training dataset includes all combinations of operand lengths (i,j) up to a maximum length k, with 20 million stratified samples ensuring balanced representation across all length pairs.

For input representation, we combine Fourier Number Embeddings (FoNE) with the Abacus method McLeish et al. (2024a). That each digit is embedded with FoNE. Training is conducted using a language model cramming approach (Geiping & Goldstein, 2023), constrained to 8 exaFLOP (equivalent to 24 hours of training on a single Nvidia RTX A6000 GPU).

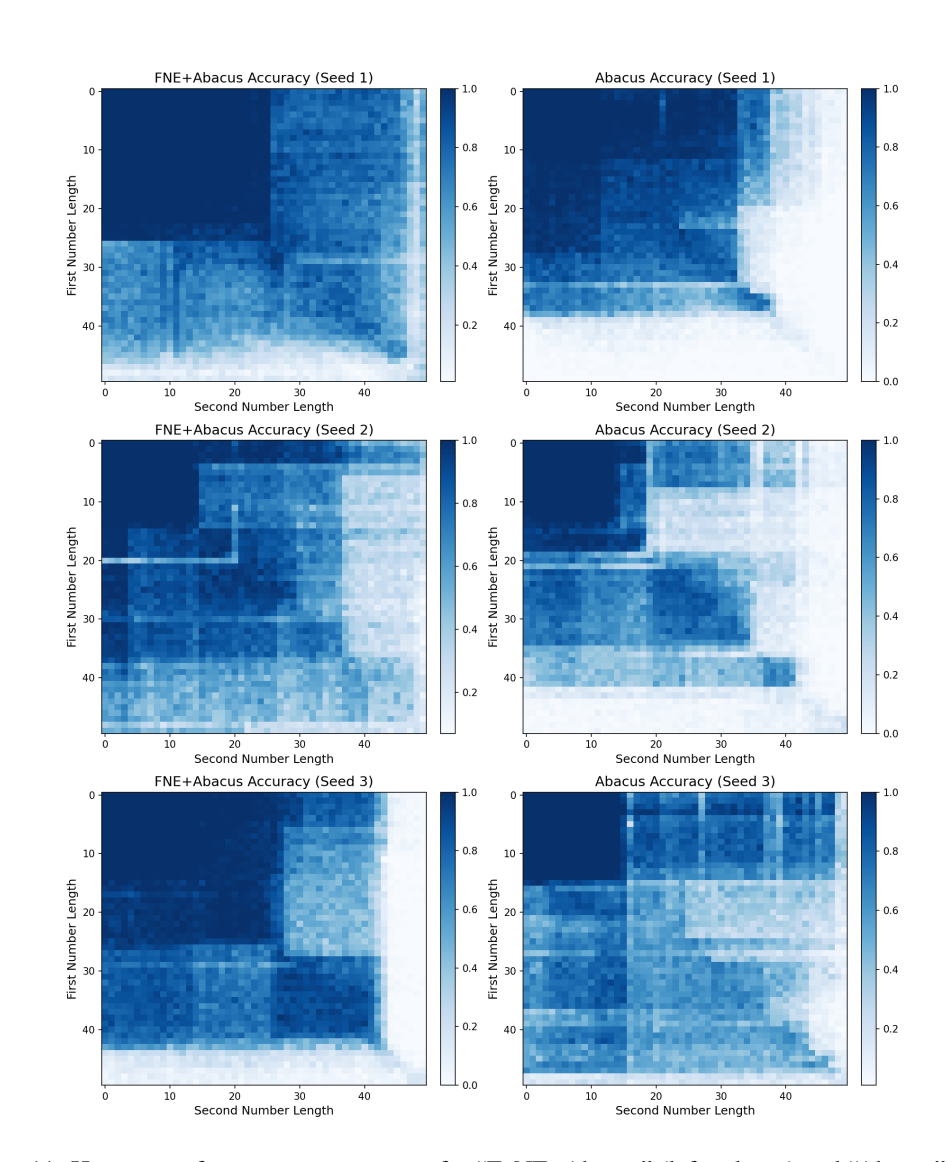


Figure 11: Heatmaps of accuracy percentages for "FoNE+Abacus" (left column) and "Abacus" (right column) across three different random seeds. Each heatmap represents accuracy as a function of the first and second number lengths, with lighter blue shades indicating higher accuracy. The color scale ranges from white (low accuracy) to blue (high accuracy). These visualizations highlight FoNE can combine with Abacus to improve performance.

We train and evaluate the models across three runs, each with a different random seed, as shown in Figure 11. Results indicate that incorporating FoNE enables the Abacus method to achieve better generalization and higher accuracy.

H CONTINUE PRETRAINING LLMs WITH SIMPLIFIED FONE

In this section, we demonstrate that our FoNE token embedding can be merged with any existing LLM with slight continual pretraining. We made a simplification of FoNE where instead of override all the number embeddings which could make continual pretraining harder, we build the simplified FoNE on top of existing BPE tokenization. For example, an number in the digit-wise form $x=a_0a_1\cdots a_k$ will be first grouped into subword by BPE tokenization $\text{BPE}(x)=(a_0a_1a_2),(a_3a_4a_5),\cdots,(\cdots a_k)$. We compute FoNE embedding of each subword, and continual pretrain a linear projection layer from the FoNE embedding space to the original token embedding space to align the embeddings similar to vision language model's alignment phase.

Table 8: A simplified version of FoNE improves model's zero-shot arithmetic abilities without sacrificing language abilities.

TASK	REGULAR	FoNE (Simplified)
4-digit addition	51.35%	59.00%
4-digit subtraction	29.60%	39.90%
5-digit addition	29.40%	35.75 %
5-digit subtraction	24.95%	33.95 %
MMLU	38.10%	38.21%

Dataset. We continual pretrain both the original **Llama-3.1-1B** model and our FoNE adapted version on 15B tokesn from MegaMath-Web-Pro (Zhou et al., 2025) and evaluated on arithmetic tasks from Brown et al. (2020) and on MMLU (Hendrycks et al., 2021).

Results. As shown in Table H, this simplified version of FoNE can improve model's zero-shot arithmetic with larger number of digits. Moreover, the lanaguge abilities evaluated by MMLU are not affected.

I MORE DETAILS ON EXPERIMENTAL SETUP

In this section, we provide the experiments settings that we used in the Section 4.1.

Learning rates were determined through an extensive search, with the best rates selected separately for each method based on validation performance. Final training hyperparameters include a learning rate of 0.005 for regular and FoNE methods, and 0.0001 for the xVal method, a batch size of 512, and 100 epochs. The fine-tuning process required less than 10 hours, while training from scratch took less than 3 days.

Dataset	Train Size	Validation Size	Test Size
6-digit decimal addition	720,000	80,000	200,000
6-digit integer addition	720,000	80,000	200,000
5-digit integer subtract	720,000	80,000	200,000
3-digit integer multiplication	360,000	40,000	100,000
4-digit integer multiplication	720,000	80,000	200,000
classification	720,00	80,00	200,00

Table 9: Dataset Sizes for Training, Testing, and Validation

Dataset	Model Size for Varying Data Size	Data Size for Varying Model Size
6-digit decimal addition	37.55M	200,000
6-digit integer addition	37.55M	200,000
5-digit integer subtract	37.55M	200,000
3-digit integer multiplication	37.55M	360,000
4-digit integer multiplication	37.55M	360,000
4-digit integer multiplication	37.55M	360,000
classification	37.55M	50,000

Table 10: Dataset and Configuration Sizes for Model and Data Variation Experiments

I.1 ABLATION STUDY

In this section, we present the mispredictions of the model trained with an FoNE, where the periods are multiples of 5 instead of 10. Table 12 demonstrates that, for each digit, the mispredictions consistently deviate from the true labels by 5.

We also present the model's mispredictions in Table 13, where each digit is encoded into a separate dimension of the embedding. For example, the number 567 is represented as [5, 6, 7]. During training,

Model	Hidden Size	Intermediate Size	# Hidden Layers	# Attention Heads	# Key-Value Heads
1	64	256	1	4	2
2	128	512	2	4	2
3	192	768	3	6	3
4	256	1024	4	8	4
5	320	1280	5	8	4
6	384	1536	6	8	4

Table 11: Model Configuration Table

Table 12: Mispredictions in the Final Evaluation with when we embed each digit with only mod 5.

Index	Predicted Value	Actual Value
1	934.03	934.585
2	3.009	558.509
3	912.311	917.366
4	6201.003	1756.008
5	1240.34	1290.84

we compute the RMSE loss between the last hidden states and the labels. During prediction, we interpret each entry in the last hidden state as a single digit.

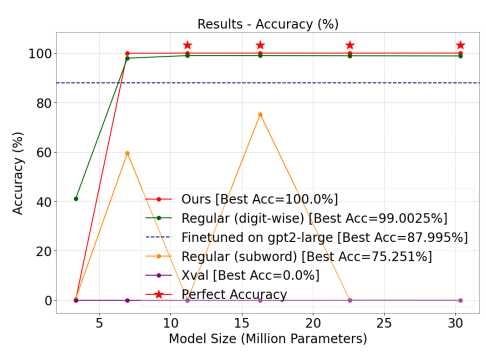
Table 13: Mispredictions in the Final Evaluation when directly encoding numbers into their embeddings.

Index	Predicted Value	Actual Value
1	883.888	993.999
2	787.878	898.989
3	888.758	989.759
4	748.785	849.895
5	677.677	688.788
10	1179.488	1189.499

J REPLICATING RESULTS ON GPT2-LARGE BASED MODEL

We conduct the same experiments on decimal addition using a GPT-2 Large-based model. The results indicate that changing the model architecture does not affect the outcomes. For instance, GPT-2 Large employs LayerNorm, while Llama 3.2 uses RMSNorm.





- (a) 6-digit decimal addition: Accuracy vs. Training Data Size
- (b) 6-digit decimal addition: Accuracy vs. Model Size

Figure 12: We train GPT2-Large from scratch with random initialization using different number embedding methods on 6-digit decimal addition. The test accuracy is compared across varying data sizes and model sizes.

K R^2 Comparison for Different Arithmetic Tasks

xVal Golkar et al. (2023) performs well on the \mathbb{R}^2 metric

$$R^{2} = 1 - \frac{\sum_{i=1}^{n} (y_{i} - \widehat{y}_{i})^{2}}{\sum_{i=1}^{n} (y_{i} - \overline{y})^{2}},$$

because it uses RMSE as its loss function. However, we demonstrate that FoNE outperforms xVal on \mathbb{R}^2 in most tasks. We show the final \mathbb{R}^2 on test dataset in our experiments(Section 4.2).

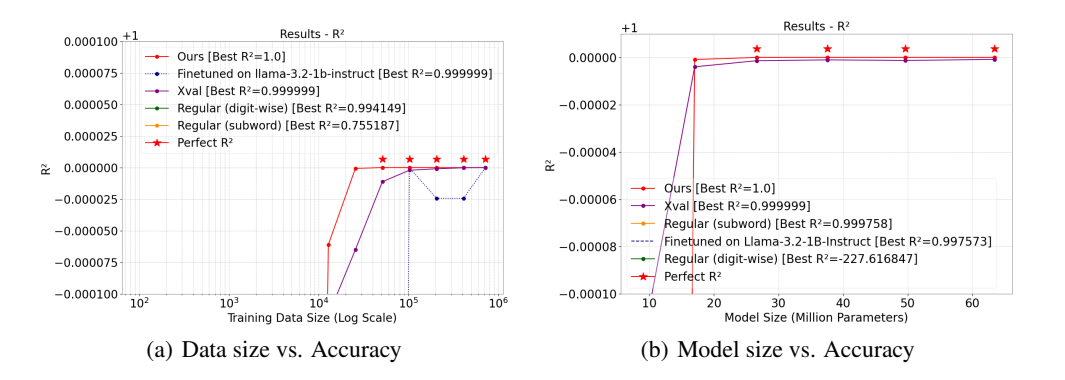


Figure 13: Comparison of \mathbb{R}^2 trends for 6-digit decimal addition with respect to model size and data size.

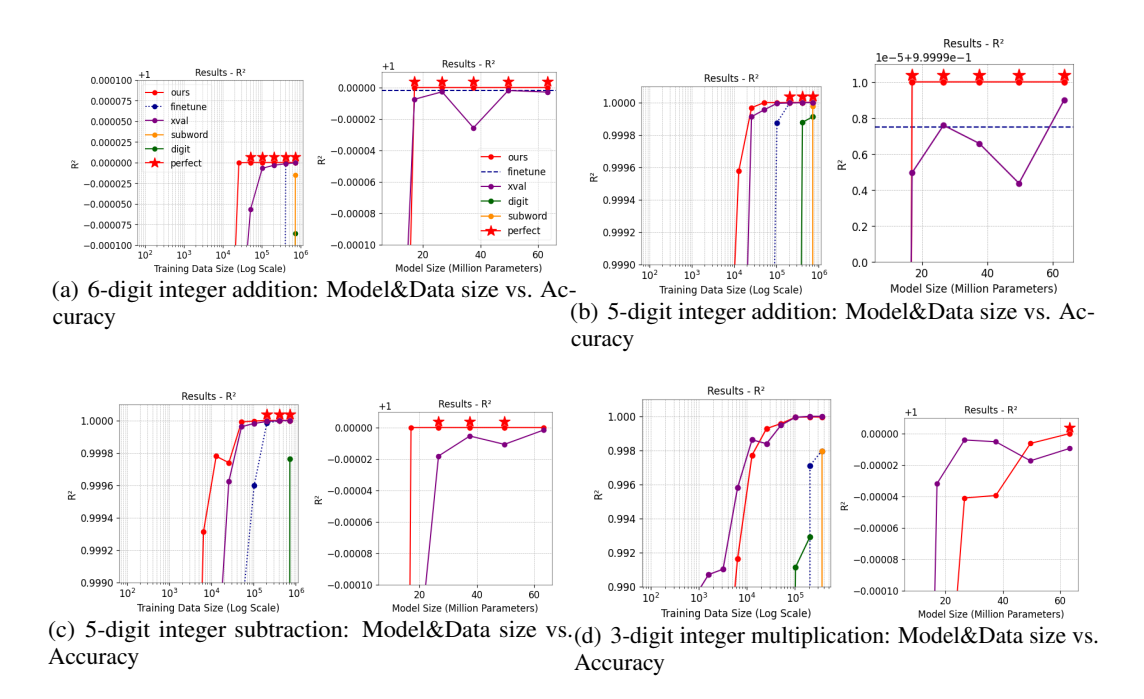


Figure 14: Comparison of \mathbb{R}^2 trends for various arithmetic tasks with respect to model size and data size.

THE USE OF LLMS

LLMs were used only to polish language, such as grammar and wording. These models did not contribute to idea creation or writing, and the authors take full responsibility for this paper's content.